



Thermal decomposition and spectroscopic investigation of a new aqueous glycolato(-peroxo) Ti(IV) solution–gel precursor

Christopher De Dobbelaere^a, Jules Mullens^a, An Hardy^{a,b}, Marlies K. Van Bael^{a,b,*}

^a Hasselt University, Institute for Materials Research, Inorganic and Physical Chemistry, Agoralaan Building D, B-3590 Diepenbeek, Belgium

^b IMEC vzw, Division IMOMECE, Agoralaan Building D, B-3590 Diepenbeek, Belgium

ARTICLE INFO

Article history:

Received 24 January 2011

Received in revised form 14 March 2011

Accepted 24 March 2011

Available online 5 April 2011

Keywords:

Aqueous solution–gel

Titanium precursor

TiO₂

TGA–MS

TGA–FTIR

Glycolic acid

ABSTRACT

A new aqueous solution–gel precursor based on water soluble glycolato(-peroxo)–Ti(IV) complexes is developed for the preparation of TiO₂ films. With regard to the decomposition of complexes towards oxide formation, it is important to gain insight in the chemical transformations inside the precursor during thermal treatment. Therefore, the thermo-oxidative decomposition pathway of a gel obtained by slow evaporation of the precursor solution is described based on hyphenated thermogravimetric analysis with Fourier transform infrared spectroscopy (TGA–FTIR) and mass spectrometry (TGA–MS). Pure glycolic acid is used as a reference system for this study. By varying the molar glycolic acid to Ti(IV) ratio, the thermal decomposition of the gel can be drastically shortened and the profile's course changed. Gel structure and chemical changes in the gel upon heating are also studied by means of off-line FTIR. A unidentate coordination of the titanium(IV) ion by the carboxylate group of the glycolato ligands and the involvement of the hydroxyl group is confirmed. Phase formation at certain points in the thermal decomposition is studied by X-ray diffraction and Raman spectroscopy. Finally, it is proven that the new precursor is a valuable candidate for the deposition of low carbon containing solution–gel films which can ultimately be converted into smooth and uniform TiO₂ films.

© 2011 Elsevier B.V. All rights reserved.

1. Introduction

Titanium dioxide (TiO₂) is a versatile material in current research and industry. Because of its physicochemical and physical properties, it is proven useful in many applications such as photovoltaic cells [1], gas sensors [2], self-cleaning coatings [3], photocatalysts [4], etc. For all practical applications, phase purity, morphology and surface area are crucial parameters towards the performance of the designed device. Anatase, brookite and rutile are the commonest TiO₂ phases at room temperature and atmospheric pressure and are obtained by different physical or chemical synthesis pathways. Chemical solution synthesis usually starts from a precursor solution in which organic compounds are applied as ligands or chelating agents that are bonded to the metal ion, protecting it from unwanted side reactions and controlling the reactions leading to a homogeneous chemical network. Different synthesis conditions can lead to the preferential formation of one of the common (meta) stable phases. The same holds for the morphology, which can be controlled by varying the precursor system

and the applied processing conditions. Both effects have already been demonstrated by several researchers [5–8]. Tomita et al. [5] for example showed that by varying the kind of hydroxycarboxylic acid applied in the synthesis of water-soluble Ti(IV) complexes, TiO₂ nano-particles with a different shape or crystalline phase can be obtained after identical hydrothermal treatments.

Not only for pure TiO₂ phases, but also in the synthesis of more complex oxide systems, Ti precursors (and others) play an important role. In electroceramic Ti containing oxides such as lead (zirconate) titanate, barium (strontium) titanate or Bi₄Fe₂TiO₁₂ obtained from sol–gel processing, all constituent metal ions influence phase formation and morphology of the obtained material. This influence is (co)related to the organic environment that surrounds the metal ions when introduced into the chemical system. As shown for PbTiO₃ films, the functional groups surrounding the lead ion influence both the thermal decomposition of the precursor and the obtained grain sizes in thin films [9]. In addition to morphology, the carbon content inside the precursor system can influence the electrical properties of the obtained functional films. Significantly lower gate leakage current densities are obtained as the carbon content in the precursor is lower, as demonstrated by electrical measurements on spin coated high-κ films [10].

With the aim of developing convenient, non-toxic and environmentally benign precursor systems for the sol–gel synthesis of titanium containing (multi) metal oxide films and powders, the

* Corresponding author. Tel.: +32 11 26 83 07; fax: +32 11 26 83 01.

E-mail addresses: christopher.dedobbelaere@uhasselt.be (C. De Dobbelaere), jules.mullens@uhasselt.be (J. Mullens), an.hardy@uhasselt.be (A. Hardy), marlies.vanbael@uhasselt.be (M.K. Van Bael).

synthesis and study of new water-soluble titanium(IV) compounds has received a lot of scientific interest [5,6,11–14]. These aqueous systems are usually based on water compatible α -hydroxy carboxylato metal complexes. Herein, multidentate ligands stabilize the central metal ion against hydrolysis and condensation in a wide pH range and allow interlinking of complexes by, e.g., ammonium-carboxylato bridging. Using these systems, acidic solutions or moisture sensitive alkoxide systems, incompatible with other systems or difficult to handle, can be avoided. Citric acid ($C_6H_8O_7$) is a common chelating agent that has already been employed in combination with other ligands to fabricate numerous citrato(-peroxo) based mono metal ion precursors [12,15–20]. However, citric acid has a molecular mass of 192 g mol^{-1} and counts at least 6 carbon atoms per metal ion in the complex.

By lowering the carbon content intrinsically present in the precursor system, any carbon pernicious for the properties of the (multi) metal oxide after calcination can be avoided. Also, by keeping the carbon content low, redundant long or high thermal decomposition steps might be avoided, keeping the thermal budget as low as possible. In view of this reduction, glycolic acid is considered a worthy alternative. Glycolic acid ($OH-CH_2-COOH$) is the smallest α -hydroxy acid possible, non-toxic and readily available. It has 2 functional groups: $-COOH$ and $-OH$, a molar mass of 76 g mol^{-1} and counts only 2 carbon atoms per molecule. Aqueous complexes based on glycolic acid ligands have already been synthesized and characterized for several metal ions, e.g. Mo(VI) [21], Cu(II), Zn(II) and Cd(II) [22], V(V) [23] and several lanthanides(III) [24] plus Th(IV) [25]. Sol-gel systems based on aqueous glycolato complexes of Ni(II), Fe(III) and Cu(II) have even been used for the preparation of $NiFe_2O_4$ nanoparticles [26] and $CuNi_{1-x}Fe_xO_y$ nanocomposites [27]. Nevertheless, the very first publication on water soluble Ti(IV) complexes based on glycolic acid only appeared in 2006 and reported on the targeted hydrothermal synthesis of phase pure anatase, brookite or rutile TiO_2 particles [6]. Later more publications regarding synthesis of TiO_2 powders from these complexes followed [5,28].

The realization of alternative precursor systems enlarges the pool of routes that can lead to the fabrication of new or common oxides or phases after thermal-oxidative decomposition. Understanding the thermo-oxidative decomposition pathway of the applied precursor systems is therefore an important aspect that needs an in depth investigation.

In the current work, a new aqueous glycolato(-peroxo)-Ti(IV) precursor route for the synthesis of titania films is presented. The effects of different glycolic acid (GA) to Ti(IV) molar ratios and the presence of peroxo ligands on the thermal decomposition have been examined. Evolving gases, released during the decomposition of a 2:1 GA:Ti(IV) precursor gel, are investigated and the chemical structure and phase of gels treated at different temperatures are studied. Finally, the microstructure and phase of a deposited film are analyzed. This fundamental study contributes to a better understanding of the decomposition of aqueous α -hydroxy carboxylato metal complexes towards oxide formation and offers an insight into the thermal treatment necessary to obtain films with an optimized morphology.

2. Experimental

2.1. Materials and reagents

Starting materials for the synthesis of the precursor solutions are liquid Ti(IV)-isopropoxide ($[(CH_3)_2CHO]_4Ti$, Acros Organics, 98+%), glycolic acid (GA, $C_2H_4O_3$, Acros Organics, 99%), hydrogen peroxide (H_2O_2 , Acros Organics, 35 wt.% in H_2O , for analysis, stabilized) and ammonia (NH_3 , Merck, 32% in H_2O , extra pure). The solvent for

precursor preparation and dilution is Milli-Q water with a resistivity of $18\text{ M}\Omega\text{ cm}$. All filtrations are carried out at room temperature using Pall Life Sciences Supor[®] 100 filters with $0.1\text{ }\mu\text{m}$ pore sizes.

2.2. Aqueous solution-gel synthesis

Aqueous glycolato(-peroxo) Ti(IV) precursors with a 0.7 M Ti(IV) concentration are prepared as follows: 22 mL Ti(IV)-isopropoxide is first hydrolyzed in 300 mL of water. While adding the metal alkoxide to the water, the solution is firmly stirred to optimally disperse the obtained hydrolysis product. The white precipitate (hydrated titanium oxide) is then washed with copious amounts of water (800 mL at least) to remove any residual isopropanol (2-propanol) formed during hydrolysis [16]. This washing step is done while stirring the filtrand over $0.1\text{ }\mu\text{m}$ filtration paper. After filtration, the solid precipitate is transferred to a 250 mL round bottom flask. Glycolic acid is then added to this same flask according to the desired glycolic acid (GA) to Ti(IV) molar ratio (e.g., 16.77 g for a 3:1 GA:Ti(IV) molar ratio). If so desired, H_2O_2 is added in a 1.2:1 H_2O_2 :Ti(IV) molar ratio (7.6 mL) for the peroxide containing precursor or is replaced by 20 mL of H_2O for the peroxide-free precursor. After mixing the reagents, the obtained suspension is refluxed for 22 h at 80°C . In case a solid gel or viscous solution is obtained after reflux (GA:Ti(IV) ratio 2:1 and lower), 20 mL H_2O and an additional stir bar are added prior to further stirring (30 min). Then, ammonia is added dropwise to the acid solution to obtain an aqueous precursor at pH 7. The solution is then refluxed for 30 min at 80°C to obtain a clear solution. If necessary, the pH is adjusted to 7 again after reflux. Finally, the solution is filtrated and diluted to 100 mL to obtain a clear aqueous glycolato(-peroxo)-Ti(IV) precursor. The precursor is transparent yellow to orange (hydrogen peroxide added) or colorless (free of hydrogen peroxide) and stable against precipitation for at least several months.

2.3. Gel preparation

Amorphous, hygroscopic gels of the obtained glycolato(-peroxo) Ti(IV) precursor solutions are obtained by drying a few drops of the aqueous solutions on a watch glass at 100°C in an air-flushed furnace for at least 24 h. The higher the glycolic acid to Ti(IV) molar ratio, the more viscous and syrupy the obtained transparent wet gels (especially the 4:1 GA:Ti(IV) gel). Low ratio gels are dry and brittle.

A metal free ammonium glycolato transparent glassy gel is prepared for comparison. This reference solution is obtained by dissolving glycolic acid in water, adjusting the pH to 7 with ammonia and diluting it to $\sim 0.4\text{ M}$. No reflux steps are necessary to obtain a clear, transparent solution. A dry gel is obtained after drying a few drops in an air-flushed furnace (24 h, 100°C).

2.4. Film deposition

A 3 layered titanium dioxide film is prepared by spin coating a 0.4 M 1:1 glycolato-Ti(IV) precursor solution onto a SPM/APM chemically cleaned [29] $SiO_2(1.2\text{ nm})/Si$ substrate. After coating (30 s, 3000 rpm, 1000 rpm/s), the as deposited wet film is treated on 3 different hot plates (in static air) as follows: 2 min at 180°C , 2 min at 300°C and 2 min at 600°C . This complete cycle is repeated 2 times prior to a final annealing step at 650°C for 30 min (preheated tube furnace, 500 mL min^{-1} dry air).

2.5. Characterization

Thermal decomposition pathways of the different Ti(IV)-precursor gels are examined by means of thermogravimetric analysis (TGA), on-line coupled with either a mass-spectrometer

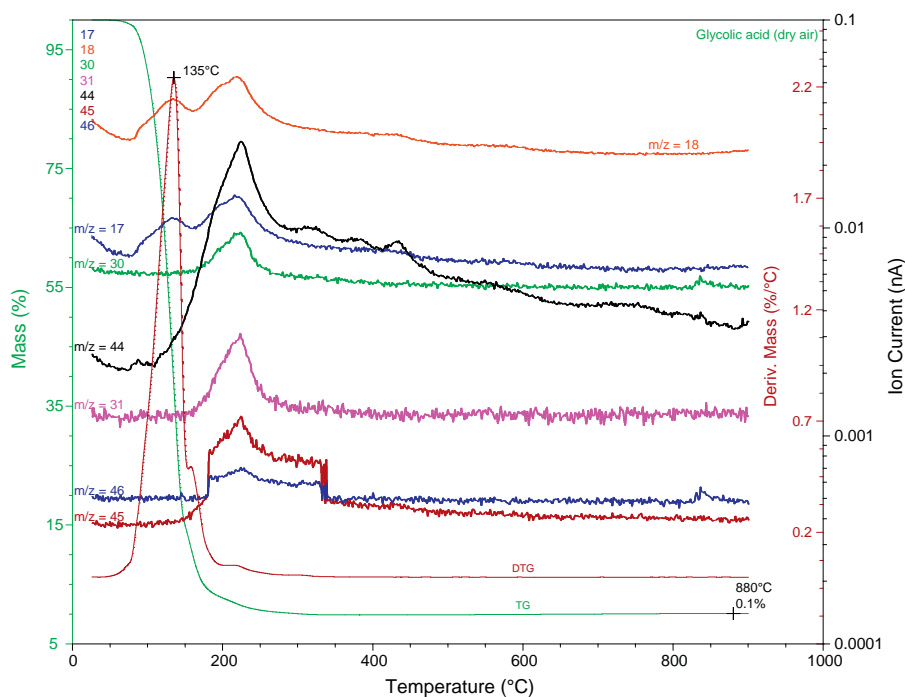


Fig. 1. TGA/DTG–MS profile of the reference glycolic acid ($C_2H_4O_3$) carried out in dry air ($10^\circ C \text{ min}^{-1}$). Only relevant fragments in the $m/z = 5\text{--}80$ region are shown (ion currents). A tentative assignment is presented in Table 1.

(MS) or a Fourier transform infra-red spectrometer (FTIR). This coupling allows the analysis of the evolved gases during heating of the gels (TGA–EGA or TGA–evolved gas analysis).

All thermogravimetric analyses are carried out on dried precursor gels ($100^\circ C$), heated from room temperature to $900^\circ C$ at a heating rate of $10^\circ C \text{ min}^{-1}$. Conventional TGA analysis is carried out on a TA Instruments SDT Q600 ($\sim 4 \text{ mg}$ of sample is used) for simultaneous TGA–DSC (differential scanning calorimetry) analysis. After sufficient flushing, the decomposition is studied in dynamic dry air or in nitrogen (100 mL min^{-1}). The inert working condition of the TGA equipment has been checked by the copper oxalate test [30]. TGA–MS analysis is carried out on a TA Instruments TGA Q5000 ($\sim 2 \text{ mg}$) coupled with a Pfeiffer Vacuum ThermoStar™ MS. Fragments formed during ionization of the evolving gas molecules are scanned in the $m/z = 5\text{--}80$ mass range in either a 25 mL min^{-1} dry air flow or a 50 mL min^{-1} helium flow. TGA–FTIR analysis is performed on a Mettler Toledo TGA/DSC1 STAR^e System ($10\text{--}20 \text{ mg}$, 100 mL min^{-1} dry air), coupled with a Bruker Vertex 70 spectrometer ($4000\text{--}600 \text{ cm}^{-1}$, 32 scans, scan velocity 20 kHz , resolution 4 cm^{-1}). The IR cell and transfer lines between the TGA and FTIR unit are held at $200^\circ C$ to avoid condensation of gases. The released gases are studied in the following spectral windows to detect relevant fragments: $2405\text{--}2335$ (CO_2), $2143\text{--}2035$ (CO), $978\text{--}947$ (NH_3), $3994\text{--}3786$ (H_2O), $3300\text{--}3215$ (HCN), $1981\text{--}1880 \text{ cm}^{-1}$ (NO) and the signals obtained are integrated to follow their time evolution.

FTIR spectra of gels and powders (powders are obtained from any gel after a temperature treatment above $\sim 180^\circ C$) are recorded at room temperature on a Bruker Vertex 70 spectrometer using KBr sample pellets ($4000\text{--}400 \text{ cm}^{-1}$, 128 scans, resolution 4 cm^{-1}). Treated gels are heated in a tube furnace to the specified temperatures and quenched to room temperature before blending with KBr. Raman spectra of powders are recorded on a Horiba Jobin Yvon micro-Raman (T64000) using a 488 nm laser as excitation source (LEXEL 95 SHG) operating at 200 mW . Powders are recorded on a Siemens D5000 diffractometer operating in $\theta\text{--}2\theta$ configuration with a focusing Bragg–Brentano geometry. A

Ge(111) monochromator selects monochromatic $Cu\text{--}K_{\alpha 1}$ radiation. Films are studied on a Bruker D8 discoverer diffractometer in $\theta\text{--}2\theta$ mode with a parallel beam geometry using a Göbel mirror (line focus, $Cu\text{--}K_{\alpha}$ radiation). The X-rays are detected by a LynxEye position sensitive detector (PSD). This 1D detector uses 192 different channels (Si strips) which all act as a separate detector. To investigate the surface morphology, scanning electron micrographs (SEM) of the deposited layers are obtained on a FEI Quanta 200FEG SEM. The metal ion concentration of the different precursors is determined by means of ICP–AES (PerkinElmer Optima 3300 DV). The pH of the precursor solutions is measured with a Schott Geräte pH–Electrode BlueLine Type 18 pH.

3. Results and discussion

3.1. TGA–MS of pure glycolic acid

Before studying the decomposition of glycolic acid based precursor gels, pure glycolic acid is examined by means of TGA–MS as a reference. Fig. 1 shows the thermal decomposition profile of pure (hygroscopic) solid glycolic acid heated at $10^\circ C \text{ min}^{-1}$ in a dry air atmosphere. From this profile, one can extract the decomposition onset at $104^\circ C$. For comparison purposes with glycolato(–peroxo) Ti(IV) precursors, thermally treated under the same conditions, it is noted that this α -hydroxy acid is almost completely decomposed around $350^\circ C$. The maximum rate of this single step decomposition is situated around $135^\circ C$. The same experiment carried out in an inert nitrogen (N_2) atmosphere results in an identical decomposition profile (not shown). This indicates that the decomposition of pure glycolic acid is thermally driven, involving no oxidative processes. Together with the thermal profile, abundant fragments released at their corresponding decomposition temperature are also presented in Fig. 1. In Table 1, a tentative assignment for the detected fragments is proposed [31,32]. Since glycolic acid belongs to the class of α -hydroxy acids, it consists of a carboxylic acid substituted with a hydroxyl group on the adjacent carbon. Typical for

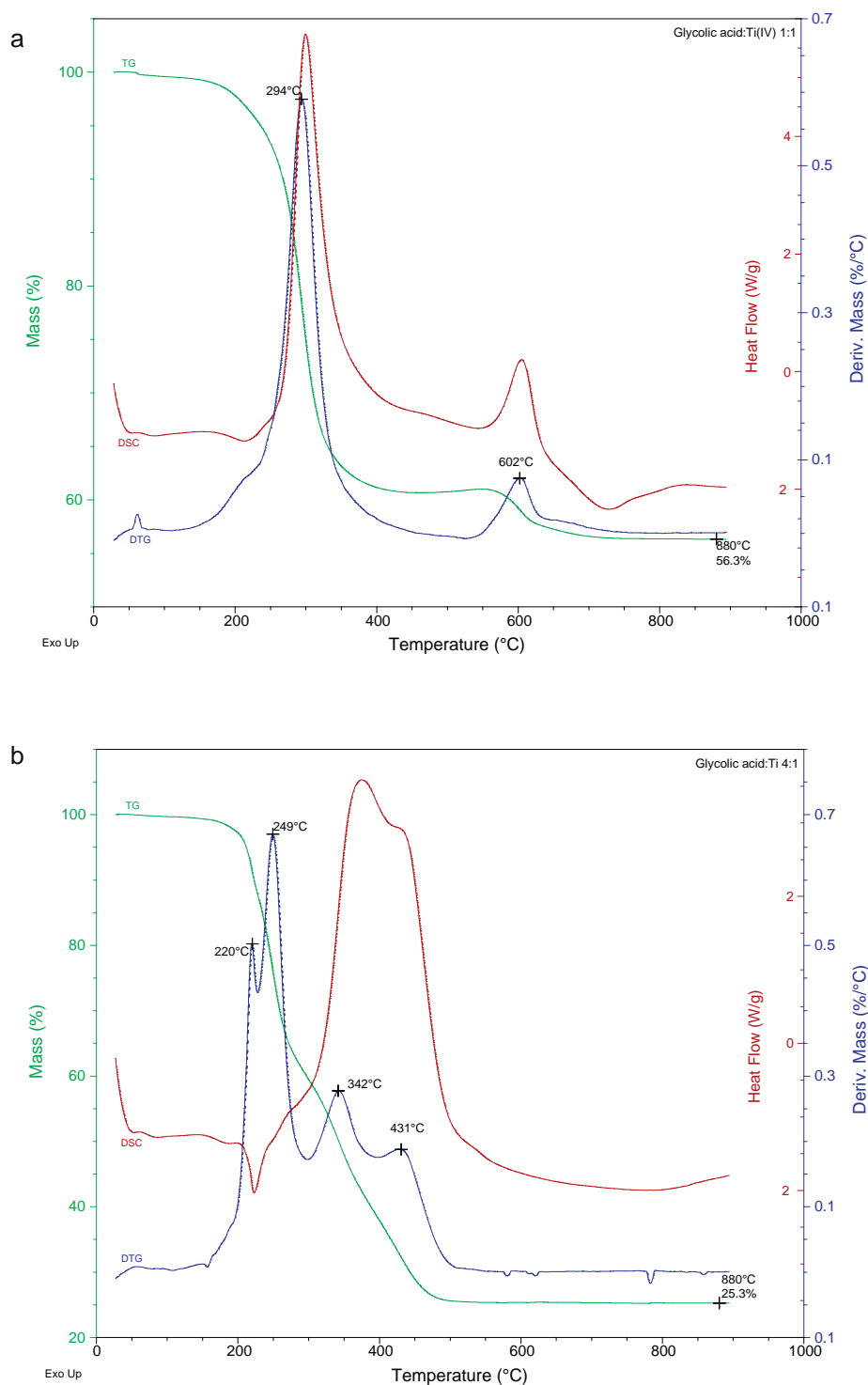


Fig. 2. TGA/DTG and DSC profile of (a) 1:1 and (b) 4:1 glycolic acid:Ti(IV) gels (no hydrogen peroxide) carried out in dry air ($10^{\circ}\text{C min}^{-1}$).

carboxylic acids is the C–CO cleavage between carbonyl and its adjacent carbon atom in a so called α -cleavage process, resulting in a representative mass fragment of $m/z = 45$ ($\text{HO-C}\equiv\text{O}^+$). The residual fragment of this cleavage has $m/z = 31$. This CH_2OH^+ fragment is associated with CH_2O^+ ($m/z = 30$) and both are characteristic fragments for primary alcohols. Other typical fragments for carboxylic acids are OH^+ ($m/z = 17$), H_2O^+ ($m/z = 18$), CO_2^+ ($m/z = 44$) and mass fragment 46 ($\text{H}_2\text{O} + \text{CO}$). Classic for primary alcohols is the elimination of water ($m/z = 18$), which is one of the first compounds to be released together with CO_2^+ ($m/z = 44$) and OH^+

($m/z = 17$). The cleavage of the bond next to the hydroxyl connecting C atom is also representative and results in the same fragments as the previously mentioned α -cleavage, i.e., $\text{HO-C}\equiv\text{O}^+$ and CH_2OH^+ . $^{13}\text{CO}_2^+$ ($m/z = 45$), CO_2^{2+} ($m/z = 22$, not shown) and C^+ ($m/z = 12$, not shown) are logically detected due to the abundant CO_2 . Other detected fragments that are less straightforward and less abundant are $\text{C}_2\text{H}_2\text{O}^+$ ($m/z = 42$, not shown) and possibly CH_2O_2 ($m/z = 46$, coincident with $\text{H}_2\text{O} + \text{CO}$). Formic acid ($m/z = 46$) is possibly formed by protonation of $\text{HO-C}\equiv\text{O}^+$ ($m/z = 45$) or as a decomposition product.

Table 1
Occurrence of mass fragments in TGA–MS of the reference glycolic acid ($C_2H_4O_3$).

m/z	Fragment(s) ^a
12	C^+
17	OH^+
18	H_2O^+
22	CO_2^{2+}
30	CH_2O^+
31	CH_2OH^+
42	$C_2H_2O^+$
44	CO_2^+
45	$HO-C\equiv O^+$, $^{13}CO_2^+$
46	$(H_2O + CO)$, CH_2O_2

^a Based on Ref. [31] (Pretsch, 2009).

It is well known that the extreme sensitivity of the MS equipment allows detecting minute mass losses that are not registered by the balance of the TGA apparatus [33]. This effect together with the narrow temperature and time window of the decomposition and the small inevitable delay between the decomposition in the TGA and the detection in the MS explain partly the late registration ($>160^\circ C$) of gases. However, the high ion current of the detected fragments around $220^\circ C$ suggests that this cannot be the only contribution. Glycolic acid is known to melt at $75^\circ C$ and evaporate around $100^\circ C$ without decomposition, as vapor-phase vibrational studies indicate [34]. Therefore, the prompt mass loss is attributed to the evaporation of the glycolic acid rather than its direct decomposition. Only in the vapor state the decomposition of the acid starts, hence the detection of fragments beyond the maximum of the DTG profile. This also explains why shape and onset of the TGA profile are indifferent to the reaction atmosphere.

3.2. Thermal decomposition of different glycolato(-peroxo)-Ti(IV) precursor gels

TGA data for studied (peroxide free) precursor gels with different glycolic acid (GA) to titanium (Ti) molar ratios measured in dry air are shown in Fig. 2 (only (a) 1:1 GA:Ti and (b) 4:1 GA:Ti are presented). As to be expected, the mass loss for the 4:1 GA:Ti ratio is the highest, i.e., 74.7% at $880^\circ C$, because a relatively higher organic content has to be decomposed when increasing the GA:Ti ratio. For the 1:1 GA:Ti ratio gel, the thermal decomposition profile can be divided into two areas. The first area stretches from room temperature to $450^\circ C$ and the second from $450^\circ C$ to the end. The major part of the decomposition of the precursor occurs around $294^\circ C$, where the highest decomposition rate is observed, as seen by the peak in the corresponding DTG profile. However, the onset of precursor decomposition already started earlier. From $230^\circ C$ to $450^\circ C$, almost forty percent of the precursor is decomposed in a single decomposition step. Single step decompositions were also observed for some crystals of divalent 1:1 glycolates, resulting in the corresponding divalent metal oxides [35]. Starting from $450^\circ C$, the mass loss is stable until $550^\circ C$, where a second small mass loss ($\sim 4\%$) occurs which was not observed for the divalent crystals reported in literature. Before this small mass loss at $550^\circ C$, Raman spectroscopy (Fig. 3a) and X-ray diffraction (Fig. 3b) indicate anatase TiO_2 , whereas at $800^\circ C$ pure rutile TiO_2 is present.

Increasing the GA:Ti ratio results in a more spread decomposition around $300^\circ C$ (not shown), with at the outside the 4:1 GA:Ti situation (Fig. 2b). The single decomposition step for the 1:1 GA:Ti ratio breaks into several steps. For the 4:1 GA:Ti gel, the decomposition peaks to a maximum around $220^\circ C$ and $249^\circ C$, $45^\circ C$ lower compared to the 1:1 ratio. More interesting is that the total decomposition now lasts until $\sim 550^\circ C$ instead of $450^\circ C$. In general, the higher the glycolic acid excess, the more steps are involved.

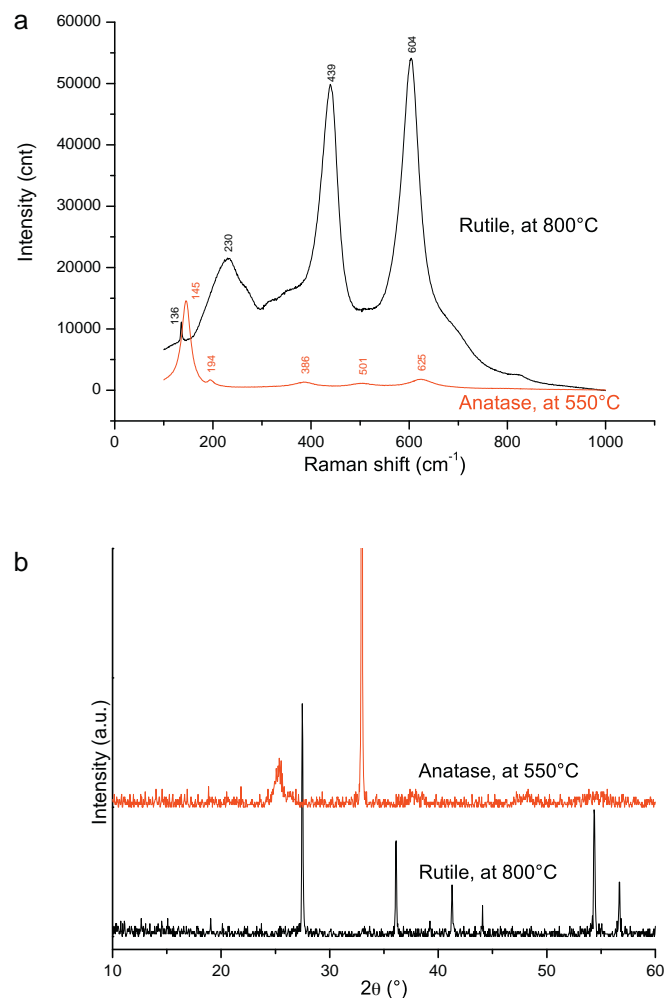


Fig. 3. (a) Raman spectrum and (b) XRD pattern of a powder obtained after stopping TGA analysis of a 2:1 glycolic acid:Ti(IV) gel at $550^\circ C$ and $800^\circ C$, resulting in anatase and rutile TiO_2 , respectively. (JCPDS anatase: 21-1272, rutile: 21-1276).

Interesting is the presence or absence of a small mass loss around $600^\circ C$ (Fig. 2). As clearly observed by the derivative signal (DTG profile), the higher the amount of glycolic acid, the smaller the mass loss at this temperature. For a 4:1 GA:Ti gel, the total thermal decomposition is complete at $550^\circ C$, whereas 1:1 is only finished around $700^\circ C$. This difference could be attributed to different heat dissipation, as seen by the heat flow in Fig. 2b. The higher GA:Ti ratio divides the quasi single exothermic step of the 1:1 ratio (at $294^\circ C$) into two events. A first endothermic step at relatively low temperature ($\sim 225^\circ C$) and a second exothermic step stretching from $310^\circ C$ till $500^\circ C$. Due to this wide exothermic process, the self-heating of the sample may extend its internal temperature above the decomposition temperature required and so perform the same decomposition at a lower temperature in the 4:1 GA:Ti gel. Indeed, when heating a 4:1 and a 1:1 GA:Ti gel to $550^\circ C$, the obtained powders have a white and purple color, respectively. This color difference might indicate that decomposition and possibly oxide formation are further evolved for the 4:1 gel. Beyond $600^\circ C$, a small endothermic step appears in the 1:1 GA:Ti gel, possibly connected to the final loss of organics since the powder's color changes from dark purple/black to white. An exothermic phase transition in the 350 – $1175^\circ C$ range is typical for any TiO_2 system, but is strongly affected by the preparation method, impurities, additives and atmosphere [36]. Increasing the amount of glycolic acid shifts the maximum of the exothermic peak to higher temper-

Table 2
Occurrence of mass fragments in TGA–MS of a 2:1 glycolic acid:Ti(IV) gel.

<i>m/z</i>	Fragment(s) ^a	Temperature region
12	C ⁺	2, 3, 4
17	OH ⁺ , NH ₃ ⁺	1, 2, 3
18	H ₂ O ⁺ , NH ₄ ⁺	1, 2, 3
22	CO ₂ ²⁺	2, 3
26	CN ⁺	3
30	CH ₂ O ⁺ , NO ⁺	3
31	CH ₂ OH ⁺	–
38	?	3
39	?	3
41	H ₂ C=C=NH ⁺	3
42	C ₂ H ₂ O ⁺	–
44	CO ₂ ⁺ , H ₂ N–C=O ⁺	2, 3, 4
45	HO–C≡O ⁺ , ¹³ CO ₂ ⁺	3
46	(H ₂ O + CO), CH ₂ O ₂ , NO ₂ ⁺	3

^a Based on Ref. [31] (Pretsch, 2009).

ature values, making the exothermic step broader. Both exothermic and endothermic events beyond 500 °C disappear for the 4:1 GA:Ti gel, which might infer another phase formation path.

Fig. 4 shows TGA/DSC (SDT) data for 2:1 GA:Ti gels where peroxide was added during precursor synthesis. The decomposition of the peroxide containing precursor is studied in (a) a dry air and (b) N₂ atmosphere (heating rate of 10 °C min⁻¹). Both mass loss and endothermic heat flow coincide until 280 °C and are linked to the endothermic decomposition of the glycolate (see Section 3.3). Exothermic processes starting at 280 °C are attributed to the oxidative decomposition of organic products previously formed and the subsequent oxidation of the metal ion [35]. This is confirmed by the gradual mass loss beyond 280 °C during pyrolysis in an inert atmosphere. Comparing both thermal profiles for a gel obtained from a 2:1 GA:Ti molar ratio solution with and without peroxide addition during precursor synthesis (Figs. 4a and 5, respectively), one could conclude that the additional O₂²⁻ ligand has no influence on the thermal stability of the glycolato(-peroxo) Ti(IV) complex, nor on the decomposition profile of the gel. Indeed the small mass difference at the end of the profile, 36.6% vs. 34.1% for the peroxide containing and peroxide free precursor, respectively, is contributed to the experimental error, as confirmed by reproducibility tests of both experiments. Results from coupled TGA–MS or TGA–FTIR could also not distinguish any difference between hydrogen peroxide free and containing systems (not shown). This means that during the further course of this study, results obtained from a Ti(IV) precursor with or without peroxide are completely interchangeable without any effect on the out coming conclusions.

3.3. Thermogravimetric analysis–evolved gas analysis (TGA–EGA) of a 2:1 GA:Ti precursor gel

Figs. 5 and 6 respectively show TGA–MS and TGA–FTIR data of a 2:1 GA:Ti (no H₂O₂) precursor gel which is thermally decomposed in a dry air atmosphere. The decomposition can arbitrarily be divided into 4 regions, centered around 100 °C, 240 °C, 330 °C and 605 °C. The second region consists of two maxima, possibly indicating that two processes are overlapping. In a helium atmosphere, the first two regions follow an identical course, showing that no oxidative processes are involved at this point (Fig. 7). This was also observed for pure glycolic acid. Gases that are released during the decomposition of a glycolato–Ti(IV) gel in dry air are characterized using MS and FTIR. An overview of the most important fragments detected by MS is given in Table 2. The assignment of released fragments is based on data previously obtained for the decomposition of pure glycolic acid and on information obtained for a citric acid based citrato–peroxo–Ti(IV) system [15,16].

From room temperature to 140 °C, only water (*m/z* = 18) and (*m/z* = 17) are released in a first endothermic process, the smallest fragment being assigned to OH⁺ or NH₃⁺. TGA–FTIR data indicates no release of NH₃. Therefore, we conclude that, as for citrato–peroxo–Ti(IV) precursors, ammonia is evolved at more elevated temperatures due to hydrogen bridging between ammonium ions and carboxylate groups [16]. This means that mass fragment 17 has to be ascribed to OH⁺ only. The mass loss in region 1 is therefore linked solely to the evaporation of residual water in the gel.

From 150 °C onwards both water and ammonia are released, which is now also confirmed by TGA–FTIR data (Fig. 6). Starting around 200 °C in region 2, CO₂ (*m/z* = 44) begins to evolve as well, reaching maxima around 205 °C and 242 °C. Since this release appears in an oxidative as well as in an inert environment (*m/z* = 44 in Figs. 5 and 7, respectively), it is concluded that this CO₂ release is due to a non oxidative process. Upon heating, the carboxylate groups in the gel start to evolve CO₂ in an endothermic decarboxylation process, typical for carboxylic acids and also observed during the decomposition of pure glycolic acid and other α-hydroxy acids [15,19]. The endothermic nature of this step is confirmed by the endothermic heat flow in a similar 4:1 GA:Ti ratio gel (Fig. 2b). Carbon dioxide starts to be released at temperatures higher than that of NH₃, see TGA–MS and TGA–FTIR data in Figs. 5 and 6, respectively. This indicates that carboxylic acid groups are formed from an ammonium carboxylate salt first and that the decarboxylation with its CO₂ loss follows hereafter: R-COO⁻ ··· H–NH₃⁺ → R-COOH + NH₃ ↑.

According to MS data, the mass loss in region 2 is solely attributed to the loss of H₂O⁺, NH₃⁺ and CO₂²⁺ with C⁺ originating from CO₂. FTIR data show that small quantities of CO (*m/z* = 28) and NO (*m/z* = 30), possibly indicating an incomplete oxidation due to local oxygen insufficiencies, are also released. They are not undoubtedly detected by MS however, due to their overlap with N₂ (*m/z* = 28) and CH₂O⁺ (*m/z* = 30).

Glycolato–Ti(IV) gels with a 1:1 GA:Ti molar ratio comprise a single decomposition step around 294 °C (Fig. 2a), however, upon augmentation of the glycolic acid excess, a new step appears at slightly lower temperature, overlapping with the former (Fig. 2b). Based on this observation, it is believed that the excess of uncoordinated ammonium glycolate is decomposed, while complexes with Ti(IV) remain intact for now. Separation of the decomposition of uncoordinated and coordinated ligands has been observed before for citrato(-peroxo)-systems of several metal ion complexes [15,16,19,20,37]. Also, the thermal decomposition of pure ammonium glycolate is finished at lower temperatures and in a single mass loss under the same experimental conditions (not shown). The loss of NH₃ can be ascribed to the decomposition of this uncomplexed ammonium glycolate, being formed out of the added ammonia and the excess of glycolic acid present in the solution. Indeed, at higher GA:Ti ratios, more ammonia is required in order to obtain a pH value of 7 during synthesis, emphasizing its abundant presence. An ammonia excess results in an additional carboxylate peak, as will be seen in the FTIR analysis of the gels (Section 3.4).

Above 280 °C (region 3) the oxidative decomposition of the gel takes place in an overall exothermic process, as shown by the exothermic peak in Fig. 2b for a similar 4:1 GA:Ti ratio gel. Two important fragments starting to evolve in this region are *m/z* = 41 and 45 (Fig. 5).

Carboxylic acids react directly with ammonia to produce amides and water upon heating. Due to this dehydration reaction, glycolamide (2-hydroxyacetamide) is a possible decomposition product for ammonium glycolate. Indicators for the formation of this amide are fragments *m/z* = 44 and 41. Besides being indicative for CO₂, *m/z* = 44 is also responsible for H₂N–C=O⁺, a fragment formed by cleavage of the C–C bond attaching the carbonyl carbon of glycolamide. The second indicator, fragment H₂C=C=NH⁺ (*m/z* = 41), is

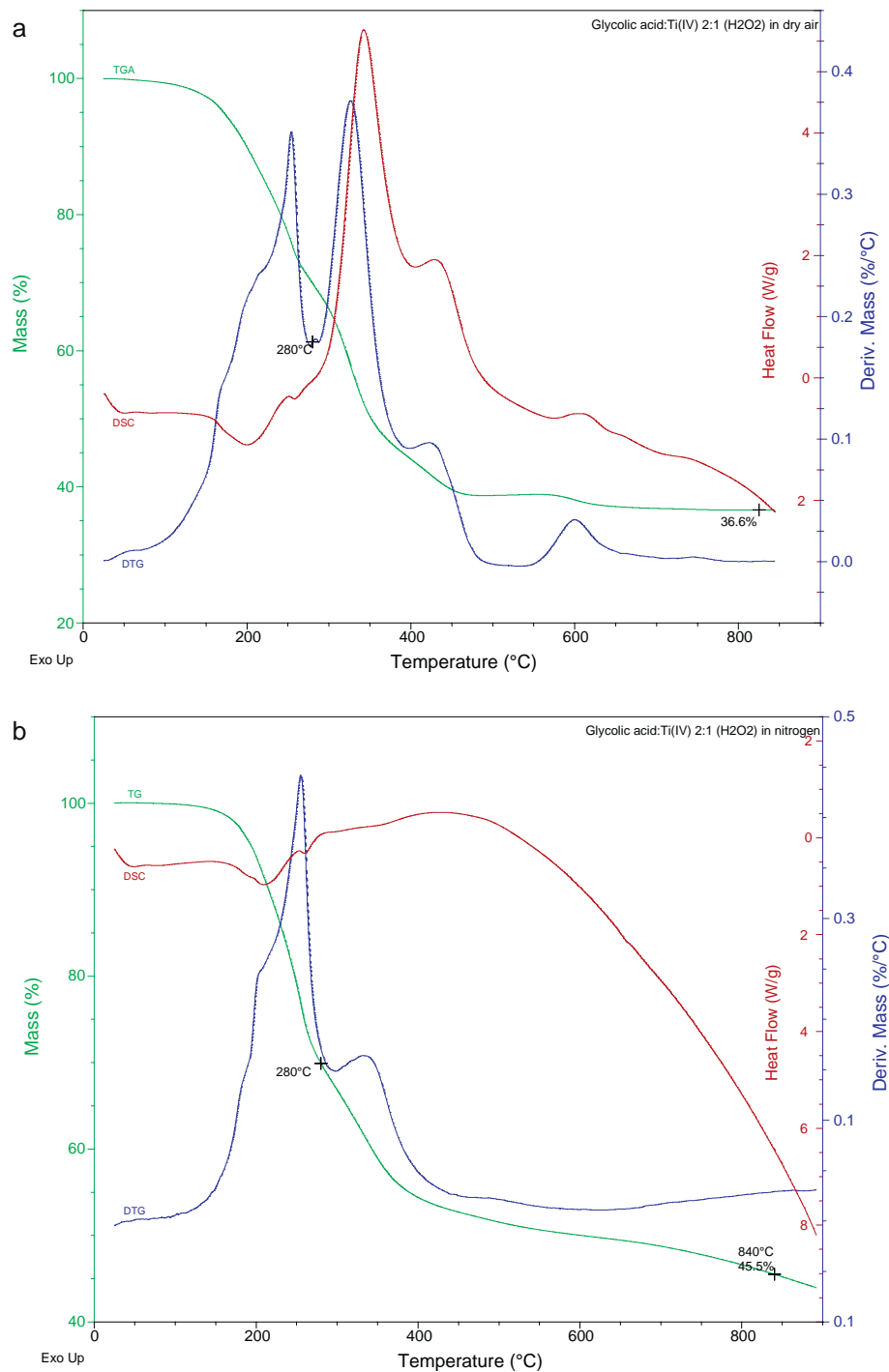


Fig. 4. TGA/DTG and DSC profile of 2:1 glycolic acid:Ti(IV) gels with hydrogen peroxide carried out in (a) dry air or (b) inert nitrogen atmosphere ($10^{\circ}\text{C min}^{-1}$).

released during treatment in both an inert and a dry air atmosphere. Thermal analysis of a similar citrato-peroxo-Ti(IV) precursor gel indicated the presence of the same $\text{H}_2\text{C}=\text{C}=\text{NH}^+$ fragment [15], being formed by a McLafferty rearrangement of an aliphatic nitrile [31]. A possible nitrile formed out of glycolamide is glycolonitrile (2-hydroxyacetonitrile). As indicated by the presence of fragment $m/z=26$ and the detection of HCN in TGA-MS and TGA-FTIR respectively, the presence of this nitrile is presumable. Since this compound however lacks a γ -H atom necessary for a McLafferty rearrangement, it is suggested that the $m/z=41$ fragment is formed from a complex intermolecular rearrangement in a glycolonitrile dimer. The existence of such a dimer [38] and the probability of

complex rearrangements in the presence of an additional hydroxyl group in short aliphatic nitriles [31] make this assumption plausible.

As mentioned for pure glycolic acid, $\text{HO}-\text{C}\equiv\text{O}^+$ ($m/z=45$) is a representative fragment for carboxylic acids, originating from an α -cleavage between the C-CO bond. Although already evolving around 180°C during decomposition of pure glycolic acid, this fragment shows up 100°C later in the glycolato-Ti(IV) precursor gel. Mass fragment $m/z=30$ can be related to CH_2O^+ or NO^+ . Even though CH_2OH^+ is related to an α -cleavage process in primary alcohols, this fragment is not detected for the glycolato-Ti(IV) gel. This is in contrast to pure glycolic acid, where the fragment is abundant.

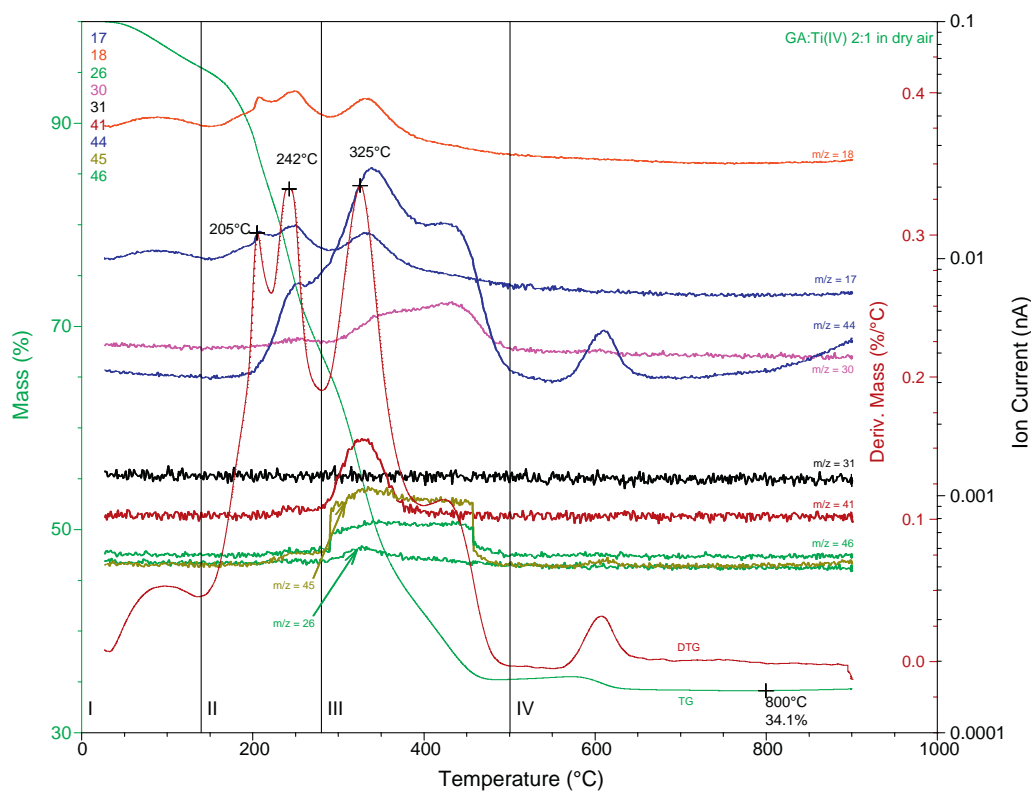


Fig. 5. TGA/DTG–MS profile of a 2:1 glycolic acid:Ti(IV) gel (no H_2O_2) carried out in dry air ($10^\circ\text{C min}^{-1}$). Only relevant fragments in the $m/z=5\text{--}80$ region are shown (ion currents). Region I: room temperature– 140°C , region II: $140\text{--}280^\circ\text{C}$, region III: $280\text{--}500^\circ\text{C}$ and region IV: 500°C –end. A tentative assignment is presented in Table 2.

The presence of CH_2O^+ indicates then either that a deprotonated hydroxyl group is involved, forming $\text{CH}_2\text{O}^{+\bullet}$ or that $m/z=30$ is solely due to nitrogen monoxide (NO^+). The $(\text{H}_2\text{O} + \text{CO})$ fragment for $m/z=46$ is typical for carboxylic acids [31] and probable since carbon monoxide is detected by means of TGA–FTIR in region 3 mainly. However, nitrogen oxide (NO_2) and CH_2O_2 are possibly also released. No reliable assignments could be made for $m/z=38$ and 39.

In general, coordinated glycolato–Ti(IV) complexes start to be decomposed in region 3. Fragments released in this region (see Table 2) indicate that organic compounds decomposed via dehydration and decarboxylation reactions are still present. This is in contrast to the glycolic acid reference, having its maximum decomposition at 135°C and being completely decomposed much earlier (before 350°C). It is thus concluded that in region 3 of the thermal decomposition profile of the glycolato–Ti(IV) gel, the decomposition of glycolato ligands coordinated to the Ti(IV) ions starts taking place. The coordination of Ti(IV) ions to glycolato ligands in this region will also be confirmed by the FTIR study in Section 3.4.

Above 500°C in region 4, only $\text{CO}_2^{+\bullet}$ ($m/z=44$) and $\text{C}^{+\bullet}$ ($m/z=12$) are released at 600°C . TGA–FTIR data confirm this final release of solely CO_2 . The final mass loss corresponds to the final decomposition of residual thermostable compounds, formed during earlier decomposition processes. As mentioned earlier, this final loss becomes smaller as the glycolic acid to Ti(IV) ratio is increased and eventually vanishes as the GA:Ti(IV) ratio becomes 4:1.

Comparing TGA–MS data obtained for a 2:1 GA:Ti(IV) precursor gel treated in dry air to data obtained in an inert helium atmosphere (Figs. 5 and 7, respectively), one clearly observes differences. Although both thermal profiles are coincident until 280°C , starting from region 3 onwards they have a different course. Since the decomposition of glycolato–Ti(IV) complexes starts around 300°C , it becomes apparent that due to the absence of oxygen glycolato ligands and fragments formed earlier during decomposition are not

completely decomposed in an inert atmosphere. The gradual mass decrease, which has even not stabilized at 900°C , indicates that the organics are only partially decomposed. At 800°C the residual mass in helium is 45.6% and the residual powder has a black color, indicating its high carbon content [8]. In dry air on the other hand, the residual mass is 34.1% and the powder is white. For pure glycolic acid, both decomposition profiles in inert atmosphere and dry air are identical.

3.4. Spectroscopic investigation of the precursor gel

To examine the functional groups that are involved in gel formation and study their behavior during thermal treatment, a spectroscopic study is carried out by means of FTIR. Therefore spectra of different glycolato–Ti(IV) gels or powders obtained after various temperature treatments are studied and compared with that of the free ligand, pure glycolic acid. A complete assignment of the absorption peaks in the glycolic acid reference is presented in Table 3. In Table 4, the infrared frequencies of the glycolato–Ti(IV) gels are reported.

The infrared spectrum of pure glycolic acid (Fig. 8a) shows a strong absorption in the $3700\text{--}2800\text{cm}^{-1}$ range due to O–H stretching modes of H-bonded hydroxyl groups ($-\text{OH}$), carboxylic acid groups ($-\text{COOH}$) and the overlapping C–H stretching modes of the methylene group. Typical for carbonyl compounds is the carbonyl stretch, $\nu(\text{C}=\text{O})$, which appears as a broad and strong IR band situated around 1734cm^{-1} . The correlated C–OH in-plane deformation, out-of-plane deformation of $-\text{COOH}$ and OC–OH stretching vibration are located at 1355 , 885 and 1385cm^{-1} , respectively. The deformation of CH_2 next to $\text{C}=\text{O}$ in $\text{CH}_2\text{--C}=\text{O}$ results in a peak at 1429cm^{-1} . The central methyl is also connected to a hydroxyl group, resulting in an O–H in-plane deformation in $\text{CH}_2\text{O--H}$ at 1234cm^{-1} and a C–O stretching vibration of $\text{CH}_2\text{--OH}$ at 1090 and 991cm^{-1} . Due to the hygroscopic nature of solid glycolic acid, the

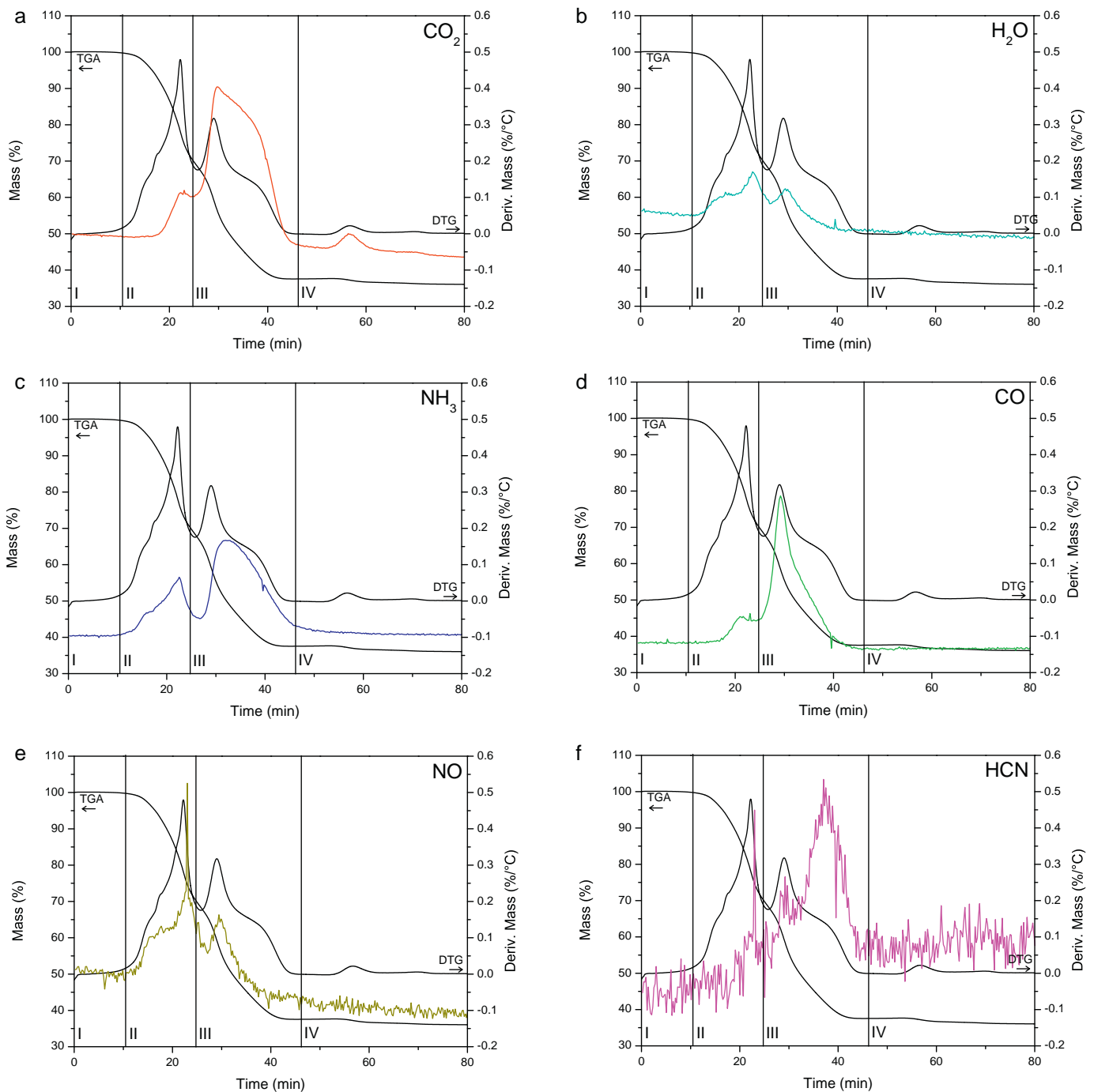


Fig. 6. TGA/DTG–FTIR profiles of a 2:1 glycolic acid:Ti(IV) gel (with H_2O_2) carried out in dry air ($10^\circ\text{C min}^{-1}$). Only integrations of relevant wavenumber windows are shown. Region I: room temperature– 140°C , region II: 140 – 280°C , region III: 280 – 500°C and region IV: 500°C -end.

broad band at 1620 cm^{-1} is assigned to the H–O–H bending of adsorbed water molecules. Other less significant peak assignments are shown in Table 3.

Apart from the characteristic modes of the ammonium cations, the IR spectra of both 4:1 and 1:1 glycolato:Ti(IV) gels show a spectral pattern similar to that of glycolic acid (Fig. 8b). In the $\nu(\text{C–H})$ and $\nu(\text{O–H})$ stretching region around 3700 – 2700 cm^{-1} , an additional broad band appears (3332 – 3100 cm^{-1}) that corresponds to $\nu(\text{N–H})$ stretching modes of the ammonium ion. All vibration modes in this 3700 – 2700 cm^{-1} area are involved in H-bond interactions, as indicated by both position and broadness of the bands. The absorption around 1400 cm^{-1} is attributed to the deformation of the NH_4^+

group. However, this peak overlaps with the CH_2 deformation of the $\text{CH}_2\text{–C=O}$ group which is present around 1429 cm^{-1} in pure glycolic acid but now appears as a shoulder at 1431 cm^{-1} .

Glycolic acid coordinates to the Ti(IV) ion during complex formation. The characteristic O–H bands of the alcohol and carboxylic acid functions clearly reveal their involvement in complexation with the Ti(IV) ions. For complexes with alcohols, it is reported that $\delta(\text{O–H})$ and $\nu(\text{OH})$ of the free ligand are red shifted and blue shifted respectively, upon coordination with the metal [39]. Indeed, $\delta(\text{O–H})$ of the in-plane deformation in $\text{CH}_2\text{O–H}$ shifts from 1234 to 1202 cm^{-1} , but the broad $\nu(\text{O–H})$ stretching stays quasi the same due to overlap with the other O–H contributions. Also, for

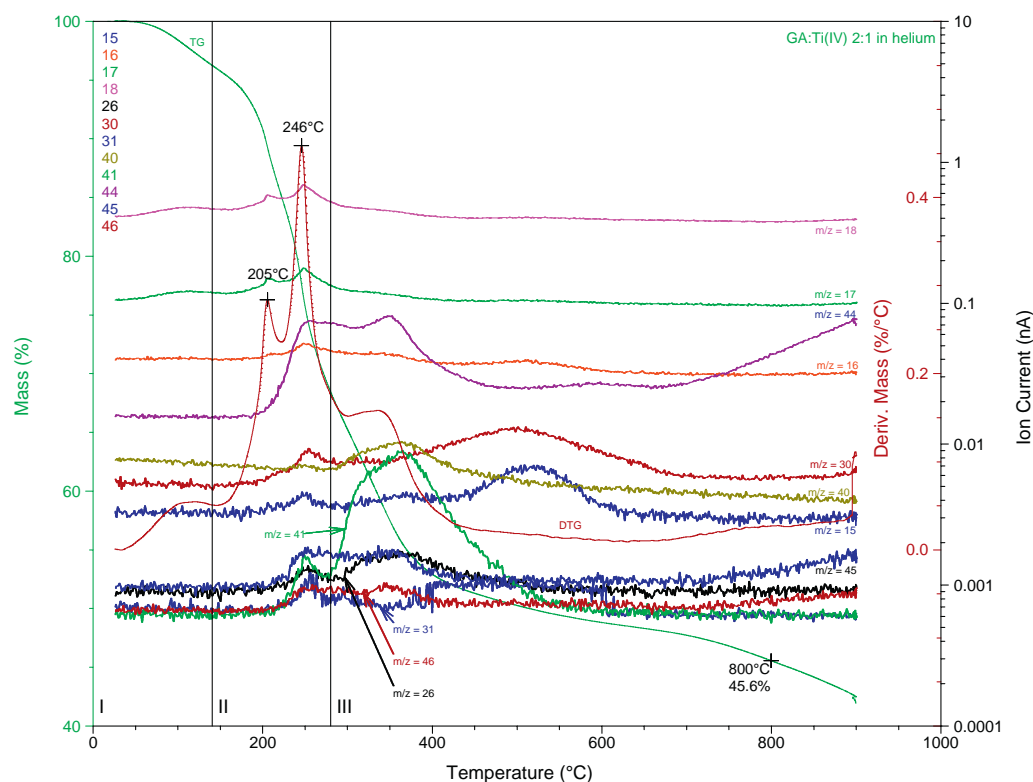


Fig. 7. TGA/DTG-MS profile of a 2:1 glycolic acid:Ti(IV) gel (no H_2O_2) carried out in helium ($10^\circ\text{C min}^{-1}$). Only relevant fragments in the $m/z=5-80$ region are shown (ion currents). Region I: room temperature- 140°C , region II: $140-280^\circ\text{C}$, region III: 280°C -end.

the 1:1 GA:Ti gel, the absorption of the $\nu(\text{O-H})$ stretching vibration around 3200 cm^{-1} is lower than that of the $\nu(\text{N-H})$ vibration around 3130 cm^{-1} , indicating its smaller contribution due to coordination with the metal ion. When maintaining an excess of glycolic acid however (4:1 GA:Ti), $\nu(\text{O-H})$ again becomes more important, having an absorption comparable to that of $\nu(\text{N-H})$. Moreover, for the 1:1 gel the contributions of the O-H in-plane deformation (1202 cm^{-1}) and OC-OH out-of-plane deformation (922 cm^{-1}) are small compared to the 4:1 gel. This indicates that less free -OH groups are available in the 1:1 GA:Ti gel due to their involvement in Ti(IV) coordination.

Glycolato-Ti(IV) gels also exhibit IR absorption bands due to the symmetric and asymmetric stretching vibrations typical for a carboxylate anion. A strong IR band at 1666 cm^{-1} can be assigned to the $\nu_{\text{as}}(\text{COO}^-)$ mode, lowered compared to the carbonyl stretching of pure glycolic acid due to coordination with the Ti(IV) ion. The symmetric stretching of the carboxylate group in a carboxy-

Table 3
Band assignments in the FTIR spectrum of pure glycolic acid.

Wavenumber (cm^{-1})	Assignment ^a
3700–3000	$\nu_{\text{O-H}}$ O-H stretching in OH and COOH
2980–2890	$\nu_{\text{C-H}}$ C-H stretching in CH_2
1734	$\nu_{\text{C=O}}$ C=O stretching in COOH
1620	$\delta_{\text{H-O-H}}$ H-O-H bending of adsorbed lattice water
1429	δ_{CH_2} CH_2 deformation in $\text{CH}_2\text{-C=O}$
1385	$\nu_{\text{C-O}}$ C-O stretching in OC-OH
1355	$\delta_{\text{C-O}}$ C-O deformation in OC-OH
1234	$\delta_{\text{O-H}}$ O-H in-plane deformation in $\text{CH}_2\text{O-H}$
1090 and 991	$\nu_{\text{C-O}}$ C-O stretching in $\text{CH}_2\text{-OH}$ (doublet)
927	$\nu_{\text{C-C}}$ C-C stretching
885	$\pi_{\text{C-O}}$ C-O out-of-plane deformation in OC-OH
727	γ_{CH_2} CH_2 skeletal vibration
663	$\pi_{\text{O-H}}$ O-H out-of-plane deformation of $\text{CH}_2\text{O-H}$

^a Based on Ref. [31] (Pretsch, 2009).

Table 4
Band assignments in the FTIR spectrum of a typical glycolato-Ti(IV) precursor gel.

Wavenumber (cm^{-1})	Assignment ^a
3650–3200	$\nu_{\text{O-H}}$ O-H stretching in OH and COOH
3332–3100	$\nu_{\text{N-H}}$ N-H stretching in NH_4^+ ^c
2980–2890	$\nu_{\text{C-H}}$ C-H stretching in CH_2
1751	$\nu_{\text{C=O}}$ C=O stretching in $\text{COO}^-/\text{NH}_4^+$
1666	$\nu_{\text{C=O}}$ Asymmetric C=O stretching in $\text{COO}^-/\text{Ti(IV)}$
1431 (sh)	δ_{CH_2} CH_2 deformation in $\text{CH}_2\text{-C=O}$
1400	$\delta_{\text{NH}_4^+}$ NH_4^+ deformation ^c
	$\nu_{\text{C=O}}$ Symmetric C=O stretching in $\text{COO}^-/\text{Ti(IV)}$
1304 + 1310	$\nu_{\text{C-O}}$ C-O stretching in OC-OH
1340 + 1354	$\delta_{\text{C-O}}$ C-O deformation in OC-OH
1202 + sh	$\delta_{\text{O-H}}$ O-H in-plane deformation in $\text{CH}_2\text{O-H}$
1090 + doublet	$\nu_{\text{C-O}}$ C-O stretching in $\text{CH}_2\text{-OH}$
922 + 930	$\pi_{\text{C-O}}$ C-O out-of-plane deformation in OC-OH
729 + 737	γ_{CH_2} CH_2 skeletal vibration
<700	δ_{COO^-} COO^- in-plane deformation
	$\pi_{\text{O-H}}$ O-H out-of-plane deformation of $\text{CH}_2\text{O-H}$
	$\pi_{\text{C=O}}$ C=O out-of-plane deformation ^b

^a Partially based on Ref. [31] (Pretsch, 2009).

^b Ref. [39] (Nakamoto, 1997).

^c Ref. [40] (Colthup, 1990).

late salt typically leads to IR absorption near 1420 cm^{-1} [40]. However, due to $\delta(\text{NH}_4^+)$ and $\delta(\text{CH}_2)$ this band is not clearly distinguishable in the spectrum. A logic assignment for $\nu_{\text{s}}(\text{COO}^-)$ is the band around 1400 cm^{-1} , which coincides with $\delta(\text{NH}_4^+)$. The frequency difference between the asymmetric and symmetric vibrations ($\Delta = [(\nu_{\text{as}}(\text{COO}^-) - \nu_{\text{s}}(\text{COO}^-))]$) is then 266 cm^{-1} , indicating a unidentate carboxylate coordination¹ of the Ti(IV) ion [39]. Based on the FTIR spectrum of a metal free 1:1 $\text{NH}_4^+:\text{GA}$ gel, the

¹ $[(\nu_{\text{as}}(\text{COO}^-) - \nu_{\text{s}}(\text{COO}^-))]$ in the sodium salt of glycolic acid is 218 cm^{-1} .

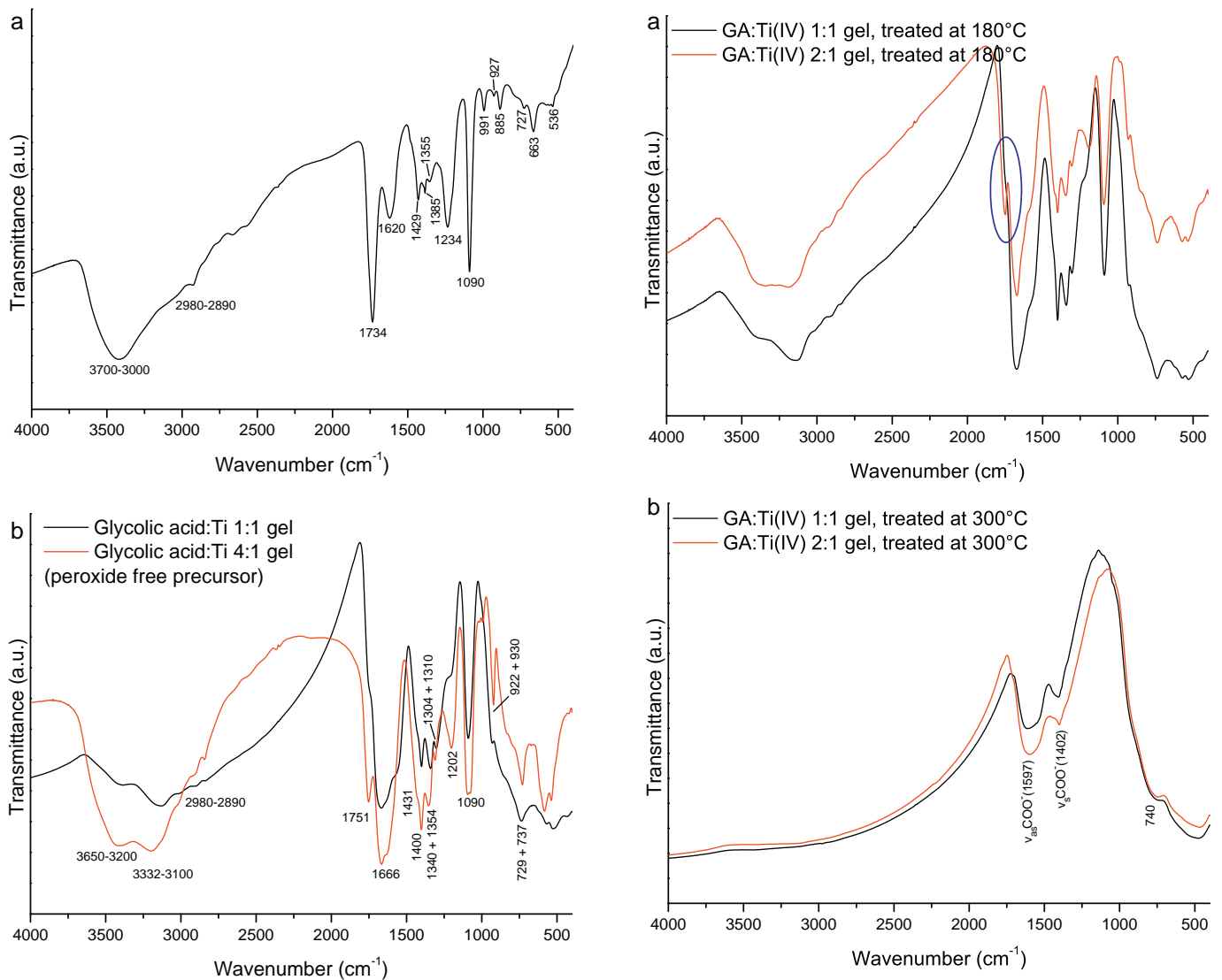


Fig. 8. FTIR spectra of (a) pure glycolic acid and (b) glycolato-Ti(IV) precursor gels with a 1:1 and 4:1 GA:Ti(IV) molar ratio (no hydrogen peroxide). Assignments are presented in Table 3 and Table 4, respectively.

sharp absorption around 1751 cm^{-1} for the 4:1 GA:Ti gel is related to $\nu(\text{COO}^-/\text{NH}_4^+)$ (not shown). This band represents the excess of glycolato groups that are not coordinated to Ti(IV). Other peak shifts due to the coordination with Ti(IV) are shown in Table 4.

Chemically, the structure of the gel consists of hydrogen bridged ammonium glycolato molecules, which build up a network, within which the metal ion complexes are bound. The carboxylate ion coordinates in a unidentate mode to the metal ion and the hydroxyl group is also involved in the coordination of the Ti(IV) ion.

FTIR spectra of glycolato-Ti(IV) gels treated at 180°C , 300°C and 600°C are shown in Fig. 9. To further study the influence of the GA excess, 2:1 and 1:1 GA:Ti gels without H_2O_2 are compared. After treatment at 180°C (in region 2 of the thermal decomposition profile), the spectra are quasi identical to those obtained after gel formation at 100°C for the 4:1 and 1:1 GA:Ti gels, respectively, (identification of the peaks see Table 4). The additional $\nu(\text{COO}^-/\text{NH}_4^+)$ stretching is also observed for the excess containing gel. Although TGA-EGA already indicated the loss of H_2O and NH_3 , these losses are not reflected in the gel structure yet. Later in region 3 at 300°C , only molecular vibrations due to carboxylate group coordinations are present: $\nu_{\text{as}}(\text{COO}^-)$ and $\nu_{\text{s}}(\text{COO}^-)$ around

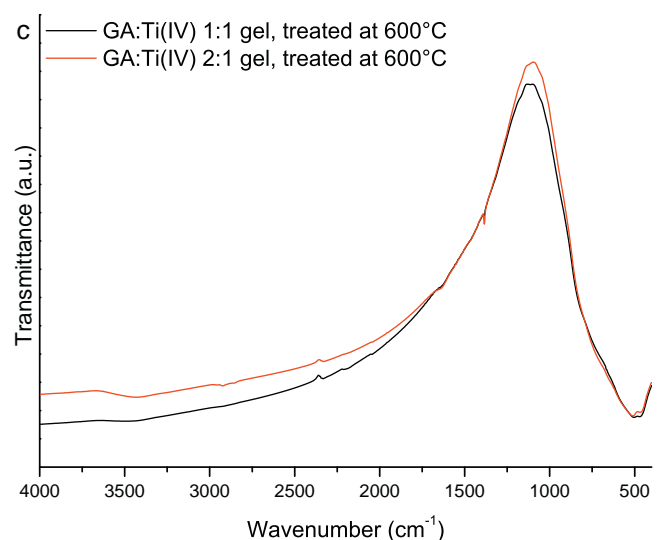


Fig. 9. FTIR spectra of peroxide free glycolato-Ti(IV) precursor gels with a 1:1 and 2:1 GA:Ti(IV) ratio treated at (a) 180°C , (b) 300°C and (c) 600°C .

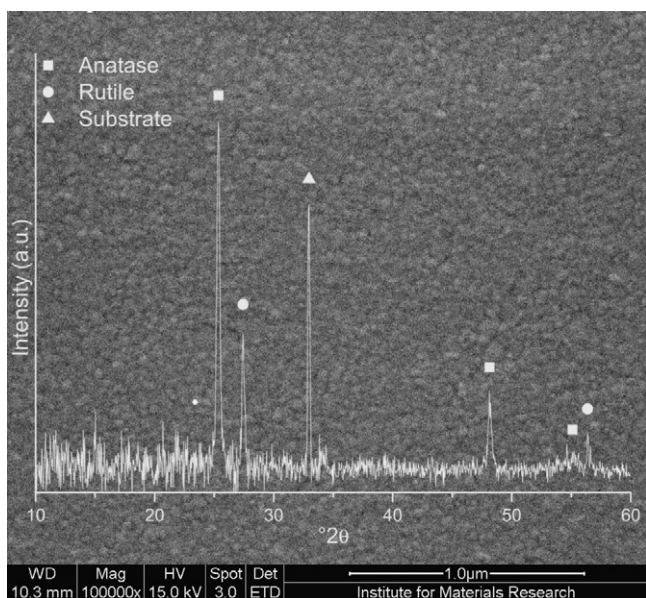


Fig. 10. SEM micrograph of a three layered TiO_2 film obtained from a 1:1 glycolato–Ti(IV) precursor. Inset: XRD pattern confirming TiO_2 formation. (JCPDS anatase: 21-1272, rutile: 21-1276).

1597 and 1402 cm^{-1} , respectively. It is not possible to reveal the origin of these coordinations due to the chemical changes inside the precursor gel during thermal treatment resulting in broad bands. As mentioned during the TGA–EGA study, the glycolato–Ti(IV) gel starts to decompose in this region. This is confirmed by the disappearance of the $\nu(\text{C–O})$ stretching of the α -hydroxy group around 1090 cm^{-1} and the $\nu(\text{COO}^-)$ shift. Since all glycolic acid excesses are already decomposed at lower temperatures, both 2:1 and 1:1 GA:Ti gels are identical now. The broad band below 700 cm^{-1} can be attributed to CH_2 skeletal vibrations of the remaining alkyl group or out-of-plane deformations originating from the carboxylate ion. Vibrations in the wide 500 cm^{-1} area possibly originate from $\nu(\text{Ti–O})$ stretching vibrations in an amorphous matrix. After treatment at 600°C all organic content is decomposed and only Ti–O stretching vibrations below 1000 cm^{-1} are observed. It is to be noted that the final organic residue which is decomposed in this area, as indicated during the thermal decomposition study, is not detectable in the FTIR spectra at 600°C . This could indicate the presence of IR inactive carbon compounds, decomposed during a final decomposition step around 600°C , as confirmed by the CO_2 ($m/z=44$) loss detected by TGA–MS and TGA–FTIR (Section 3.3).

3.5. Film deposition

To indicate the value of the aqueous glycolato–Ti(IV) precursor system (no peroxide), a three layered TiO_2 film is deposited on a SiO_2 substrate. A 1:1 GA:Ti(IV) aqueous glycolato–Ti(IV) precursor is used since this precursors intrinsically has the lowest carbon content. The microstructure of the obtained film is examined by SEM and shown in Fig. 10. A smooth, uniform and small grained microstructure is obtained. No porous areas nor cracks are observed. Phase formation is confirmed by X-ray diffraction (Fig. 10, inset). A mixture of anatase and rutile is obtained, since the final crystallization temperature for the film was 650°C . By changing the crystallization temperature to lower or higher values, phase pure anatase or rutile would be obtained, respectively. For peroxide containing Ti(IV) precursors, identical morphologies and phases are obtained (not shown).

4. Conclusion

Water-soluble precursors for Ti(IV) based on glycolic acid (GA, an α -hydroxy acid) and hydrogen peroxide as ligands to protect the ion from hydrolysis, are synthesized and their thermal decomposition is characterized. The peroxide group is no real necessity to obtain a stable solution and can be omitted. Solutions with different glycolic acid to titanium(IV) molar ratios are prepared (4:1 to 1:1 GA:Ti(IV)) and the effect of the excess glycolic acid (and the presence of peroxy ligands) on both stability and thermal decomposition is examined.

Generally, two scenarios are possible for the thermal decomposition of a glycolato(-peroxy)–Ti(IV) gel in dry air. For a 1:1 GA:Ti(IV) gel, the decomposition consists of two single steps centered around 300°C and 600°C . Since no glycolic acid excess is involved, ammonium glycolato(-peroxy)–Ti(IV) is directly decomposed in a first single step. In the second step, residual organics formed during the first step are further decomposed leaving only Ti–O bonds behind. In case the GA:Ti(IV) ratio is higher than 1:1, the decomposition pathway changes and can arbitrary be divided into 4 regions. Ammonium glycolate and glycolato(-peroxy)–Ti(IV) complexes are now decomposed in separated steps. After evaporation of residual water in the gel, decomposition of ammonium glycolate occurs. In the third step, glycolato ligands coordinated to the Ti(IV) metal start to decompose and finally, residual organics previously formed, are combusted and Ti–O bonds remain. An important discovery is that by increasing the excess of glycolic acid, the decomposition pathway can be shortened due to an excessive and wide exothermic step that allows the skipping of the final step that usually decomposes the last residual compounds.

A spectroscopic study for all glycolato(-peroxy)–Ti(IV) gels reveals that Ti(IV) is coordinated to the carboxylate group of the glycolato ligand in an unidentate fashion. FTIR also reveals the involvement of the hydroxyl group. From the third region of the decomposition on it is not possible to unambiguously identify the real coordination of the metal ion. Using complementary TGA experiments however, it can be confirmed that the glycolato(-peroxy)–Ti(IV) complexes are decomposed after all ammonium glycolate is removed.

Smooth, uniform and pure TiO_2 films are prepared to illustrate the value of this new aqueous glycolato(-peroxy)–Ti(IV) precursor. We foresee several applications for this minimally low carbon aqueous Ti(IV) precursor.

Acknowledgements

The authors acknowledge Prof. Dr. R. Carleer, G. Reggers and M. Vanhamel for many fruitful discussions regarding TGA–MS and TGA–FTIR experiments and are indebted to Dr. J. D'Haen and B. Rutens for all physical characterizations (XRD and SEM). The authors thank N. Peys for the Raman spectra. A. Hardy is a postdoctoral research fellow and C. De Dobbelaere a research assistant of the Research foundation-Flanders (FWO-Vlaanderen).

References

- [1] B. Oregan, M. Grätzel, A low-cost, high-efficiency solar-cell based on dye-sensitized colloidal TiO_2 films, *Nature* 353 (1991) 737–740.
- [2] L.R. Skubal, N.K. Meshkov, M.C. Vogt, Detection and identification of gaseous organics using a TiO_2 sensor, *J. Photochem. Photobiol. A* 148 (2002) 103–108.
- [3] A.G. Agrios, P. Pichat, State of the art and perspectives on materials and applications of photocatalysis over TiO_2 , *J. Appl. Electrochem.* 35 (2005) 655–663.
- [4] A. Fujishima, K. Honda, Electrochemical photolysis of water at a semiconductor electrode, *Nature* 238 (1972) 37–38.
- [5] K. Tomita, M. Kobayashi, V. Petrykin, S. Yin, T. Sato, M. Yoshimura, M. Kakihana, Hydrothermal synthesis of TiO_2 nano-particles using novel water-soluble titanium complexes, *J. Mater. Sci.* 43 (2008) 2217–2221.
- [6] K. Tomita, V. Petrykin, M. Kobayashi, M. Shiro, M. Yoshimura, M. Kakihana, A water-soluble titanium complex for the selective synthesis of nanocrystalline

- brookite, rutile, and anatase by a hydrothermal method, *Angew. Chem. Int.* 45 (2006) 2378–2381.
- [7] K. Yamamoto, K. Tomita, K. Fujita, M. Kobayashi, V. Petrykin, M. Kakihana, Synthesis of TiO₂(B) using glycolate titanium complex and post-synthetic hydrothermal crystal growth of TiO₂(B), *J. Cryst. Growth* 311 (2009) 619–622.
- [8] K. Yasui, T. Isobe, A. Nakajima, Preparation and photocatalytic activity of TiO₂ powders from titanium citrate complex using two-step hydrothermal treatments, *Mater. Lett.* 64 (2010) 2036–2039.
- [9] B. Malic, M. Kosec, K. Smolej, S. Stavber, Effect of precursor type on the microstructure of PbTiO₃ thin films, *J. Eur. Ceram. Soc.* 19 (1999) 1345–1348.
- [10] S. Van Elshocht, A. Hardy, C. Adelman, M. Caymax, T. Conard, A. Franquet, O. Richard, M.K. Van Bael, J. Mullens, S. De Gendt, Impact of process optimizations on the electrical performance of high-κ layers deposited by aqueous chemical solution deposition, *J. Electrochem. Soc.* 155 (2008) G91–G95.
- [11] M. Kakihana, M. Tada, M. Shiro, V. Petrykin, M. Osada, Y. Nakamura, Structure and stability of water soluble (NH₄)₈[Ti₄(C₆H₄O₇)₄(O₂)₄]·8H₂O, *Inorg. Chem.* 40 (2001) 891–894.
- [12] M. Dakanali, E.T. Kefalas, C.P. Raptopoulou, A. Terzis, G. Voyiatzis, I. Kyrikou, T. Mavromoustakos, A. Salifoglou, A new dinuclear Ti(IV)–peroxo–citrate complex from aqueous solutions. Synthetic, structural, and spectroscopic studies in relevance to aqueous titanium(IV)–peroxo–citrate speciation, *Inorg. Chem.* 42 (2003) 4632–4639.
- [13] Y.F. Deng, Z.H. Zhou, H.L. Wan, pH-dependent isolations and spectroscopic, structural, and thermal studies of titanium citrate complexes, *Inorg. Chem.* 43 (2004) 6266–6273.
- [14] M. Kakihana, K. Tomita, V. Petrykin, M. Tada, S. Sasaki, Y. Nakamura, Chelating of titanium by lactic acid in the water-soluble diammonium tris(2-hydroxypropionato)titanate(IV), *Inorg. Chem.* 43 (2004) 4546–4548.
- [15] I. Truijien, A. Hardy, M.K. Van Bael, H. Van den Rul, J. Mullens, Study of the decomposition of aqueous citratoperoxo–Ti(IV)–gel precursors for titania by means of TGA–MS and FTIR, *Thermochim. Acta* 456 (2007) 38–47.
- [16] A. Hardy, J. D'Haen, M.K. Van Bael, J. Mullens, An aqueous solution–gel citratoperoxo–Ti(IV) precursor: synthesis, gelation, thermo-oxidative decomposition and oxide crystallization, *J. Sol–Gel Sci. Technol.* 44 (2007) 65–74.
- [17] R.I. Bickley, H.G.M. Edwards, R. Gustar, S.J. Rose, A vibrational spectroscopic study of nickel(II) citrate Ni₃(C₆H₅O₇)₂ and its aqueous-solutions, *J. Mol. Struct.* 246 (1991) 217–228.
- [18] M. Kourgiantakis, M. Matzapetakis, C.P. Raptopoulou, A. Terzis, A. Salifoglou, Lead-citrate chemistry. Synthesis, spectroscopic and structural studies of a novel lead(II)–citrate aqueous complex, *Inorg. Chim. Acta* 297 (2000) 134–138.
- [19] K. Van Werde, D. Mondelaers, G. Vanhoyland, D. Nelis, M.K. Van Bael, J. Mullens, L.C. Van Poucke, B. Van der Veken, H.O. Desseyn, Thermal decomposition of the ammonium zinc acetate citrate precursor for aqueous chemical solution deposition of ZnO, *J. Mater. Sci.* 37 (2002) 81–88.
- [20] A. Hardy, K. Van Werde, G. Vanhoyland, M.K. Van Bael, J. Mullens, L.C. Van Poucke, Study of the decomposition of an aqueous metal–chelate gel precursor for (Bi,La)₄Ti₃O₁₂ by means of TGA–FTIR, TGA–MS and HT–DRIFT, *Thermochim. Acta* 397 (2003) 143–153.
- [21] A. Cuin, A.C. Massabni, Synthesis and characterization of solid molybdenum(VI) complexes with glycolic, mandelic and tartaric acids. Photochemistry behaviour of the glycolate molybdenum complex, *J. Coord. Chem.* 60 (2007) 1933–1940.
- [22] Z. Warnke, Investigation on divalent metal complexes with oxyacids in aqueous solutions.6. Potentiometric investigation on copper(II), zinc(II), and cadmium(II) complexes with glycolic acid, *Rocz. Chem.* 43 (1969) 1939.
- [23] L.L.G. Justino, M.L. Ramos, M.M. Caldeira, V.M.S. Gil, Peroxovanadium(V) complexes of glycolic acid as studied by NMR spectroscopy, *Inorg. Chim. Acta* 311 (2000) 119–125.
- [24] Z. Hnatejko, S. Lis, M. Elbanowski, Spectroscopic study of lanthanide(III) complexes with chosen aminoacids and hydroxyacids in solution, *J. Alloys Compd.* 300–301 (2000) 38–44.
- [25] T. Toraishi, I. Farkas, Z. Szabo, I. Grenthe, Complexation of Th(IV) and various lanthanides(III) by glycolic acid; potentiometric, C-13-NMR and EXAFS studies, *J. Chem. Soc. Dalton Trans.* (2002) 3805–3812.
- [26] M. Srivastava, S. Chaubey, A.K. Ojha, Investigation on size dependent structural and magnetic behavior of nickel ferrite nanoparticles prepared by sol–gel and hydrothermal methods, *Mater. Chem. Phys.* 118 (2009) 174–180.
- [27] M. Srivastava, A.K. Ojha, S. Chaubey, P.K. Sharma, A.C. Pandey, Glycolic acid assisted one-step synthesis of Cu–Ni–Fe metal oxide nanocomposites by sol–gel-combustion method: structural, spectroscopic and magnetic studies, *Mater. Chem. Phys.* 120 (2010) 493–500.
- [28] M. Kobayashi, V.V. Petrykin, M. Kakihana, One-step synthesis of TiO₂(B) nanoparticles from a water-soluble titanium complex, *Chem. Mater.* 19 (2007) 5373–5376.
- [29] M.K. Van Bael, D. Nelis, A. Hardy, D. Mondelaers, K. Van Werde, J. D'Haen, G. Vanhoyland, H. Van den Rul, J. Mullens, L.C. Van Poucke, F. Frederix, D.J. Wouters, Aqueous chemical solution deposition of ferroelectric thin films, *Integr. Ferroelectr.* 45 (2002) 113–122.
- [30] J. Mullens, A. Vos, R. Carleer, J. Yperman, L.C. Vanpoucke, The Decomposition of copper oxalate to metallic copper is well suited for checking the inert working-conditions of thermal-analysis equipment, *Thermochim. Acta* 207 (1992) 337–339.
- [31] E. Pretsch, P. Bühlmann, M. Badertscher, Structure Determination of Organic Compounds – Tables of Spectral Data, fourth ed., Springer-Verlag, 2009.
- [32] T.N. Sorrell, Interpreting Spectra of Organic Molecules, University Science Books, Mill Valley (CA), 1988.
- [33] J. Mullens, EGA – Evolved gas analysis, in: M.E. Brown (Ed.), Handbook of Thermal Analysis and Calorimetry, Elsevier Science, 1998, pp. 509–546.
- [34] D.K. Havey, K.J. Feierabend, V. Vaida, Vapor-phase vibrational spectrum of glycolic acid, CH₂OHCOOH, in the region 2000–8500 cm⁻¹, *J. Phys. Chem. A* 108 (1994) 9069–9073.
- [35] M.R. Udupa, G.K. Ramachandra, Thermal-decomposition of Mn(II), Fe(II), Co(II), Ni(II), Cu(II), Zn(II) and Cd(II) glycolates, *Indian J. Chem.* A 21 (1982) 162–163.
- [36] A. Dassler, A. Feltz, J. Jung, W. Ludwig, E. Kaisersberger, Characterization of rutile and anatase powders by thermal-analysis, *J. Therm. Anal.* 33 (1988) 803–809.
- [37] K. Van Werde, G. Vanhoyland, D. Mondelaers, H. Van den Rul, M.K. Van Bael, J. Mullens, L.C. Van Poucke, The aqueous solution–gel synthesis of perovskite Pb(Zr_{1-x}Ti_x)O₃ (PZT), *J. Mater. Sci.* 42 (2007) 624–632.
- [38] X.H. Ju, L.J. Xie, Q.Y. Xia, H.M. Xiao, Ab initio studies on intermolecular interaction of formamide and hydroxyacetone dimers, *Chem. Res. Chin. Univ.* 20 (2004) 354–357.
- [39] K. Nakamoto, Infrared and Raman Spectra of Inorganic and Coordination Compounds, fifth ed., Wiley & Sons, New York, 1997.
- [40] N.B. Colthup, L.H. Daly, S.E. Wiberley, Introduction to Infrared and Raman Spectroscopy, third ed., Academic Press, New York, 1990.